2013 IEEE/RSJ International Conference on
Intelligent Robots and Systems (IROS)
November 3-7, 2013. Tokyo, Japan

Robust Laser Beam Tracking Control using Micro/Nano Dual-Stage Manipulators

Nabil Amari, David Folio and Antoine Ferreira

Abstract— **This paper presents a study of the control problem of a laser beam illuminating and focusing a microobject subjected to dynamic disturbances using light intensity for feedback only. The main idea is to guide and track the beam with a hybrid micro/nanomanipulator which is driven by a control signal generated by processing the beam intensity sensed by a four-quadrant photodiode. Since the pointing location of the beam depends on real-time control issues related to temperature variation, vibrations, output intensity control, and collimation of the light output, the 2D beam location to the photodiode sensor measurement output is estimated in real-time. We use the Kalman filter (KF) algorithm for estimating the state of the linear system necessary for implementing the proposed track-following control approach. To do so a robust master/slave control strategy for micro/nano dual-stage manipulators is presented based on sensitivity function decoupling design methodology. The decoupled feedback controller is synthesized and implemented in a 6 dof micro/nanomanipulator capable of nanometer resolution through several hundreds micrometer range. A case study relevant to tracking a laser-beam for imaging purposes is presented.**

I. Introduction

High-precision position measurement systems based on laser beam reflection and/or transmission are commonly used in nanorobotics applications. It is composed of the optical detecting set, including the laser diode (LD), the position-sensitive detector (PSD), alignment mechanisms, and the frame structure for maintaining the optical configuration. The general problem is to focus the beam in few micrometer size spots and to control actively the beam direction to stabilize the beam at a desired location (see Fig.1). This is desirable in nanomanipulation tasks when focusing a near-infrared laser beam at a nerve cell's leading edge [1], [2], when the laser beam perfectly tracks the moving atomic force microscope (AFM) probes [3] during manipulation tasks, or when the laser beam illuminates a microobject handled by a nanogripper for material characterization [4]. Usually, the laser beam calibration is time-consuming since the laser beam could be steered manually. Precise laser beam tracking of dynamic position with high-bandwidth rejection of disturbances is required. The perturbations produced by platform vibrations, piezoelectric actuator thermal drifts, photodetector noises, brownian motion of laser beam and atmospheric turbulence are critical for the success of micro and nanomanipulation tasks. As the single photodiode sensor is currently being used only for position measurement,

N. Amari, D. Folio and A. Ferreira are with the Laboratoire PRISME EA 4229; Ecole Nationale Suprieure d'Ingnieurs de Bourges, 88 boulevard Lahitolle, 18020 Bourges, France. Corresponding author: Antoine Ferreira (Email:antoine.ferreira@ensi-bourges.fr, Tel: +33 2 4848 4079)

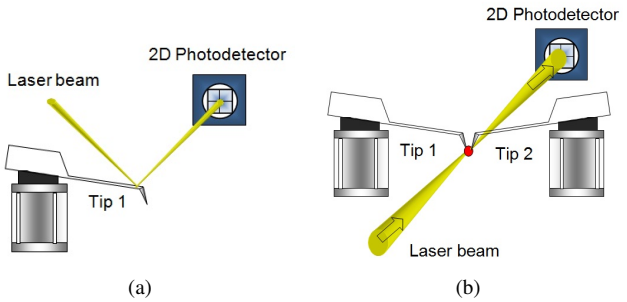

Fig. 1. High-precision position measurement based on (a) the laser beam steering (reflection), and (b) the photodetector steering (transmission) commonly used in nanomanipulation applications.

the possibility of using it for feedback control is of great interest, since this might significantly increase the overall performance and reliability of nanorobotic systems. Two laser beam tracking configurations are found in the literature, i.e. steering the laser beam or steering the photodetector. In the first case, some works propose to use fast tilt two-axis steering mirrors based on electrostatic MEMS actuators [5] or piezoelectric actuators with a fixed four-quadrant PSD. In the second case, the PSD is driven by a dual actuation system with nanomanipulators [6], or x-y linear positioning stages [7]. Whatever the technology involved, robust control of the laser beam tracking system is needed.

The purpose of this paper is to design a control system that rejects disturbances in the sense of minimizing the variance of the error in the position of the laser beam. The main idea is to track the emitting beam by processing the maximum beam intensity sensed by a four-quadrant PSD mounted on a 6 degree of freedom (dof) dual-stage micro/nanomanipulator platform. Since the pointing location of the beam depends on real-time control issues related to disturbances, the laser beam position is estimated in real-time using the Kalman filter (KF) algorithm. To do so, a robust decoupled design controller is presented based on sensitivity function decoupling design methodology. The decoupled feedback controller is synthesized and implemented in a 6 dof coupled magnetic and piezoelectric manipulation platform.

The paper is divided into five sections. Section 2 describes the experimental setup. Section 3 describes the dynamics modeling and system identification procedure and results. Section 4 describes the decoupled control design structure. Section 5 presents experimental results for the performance of the beam steering system.

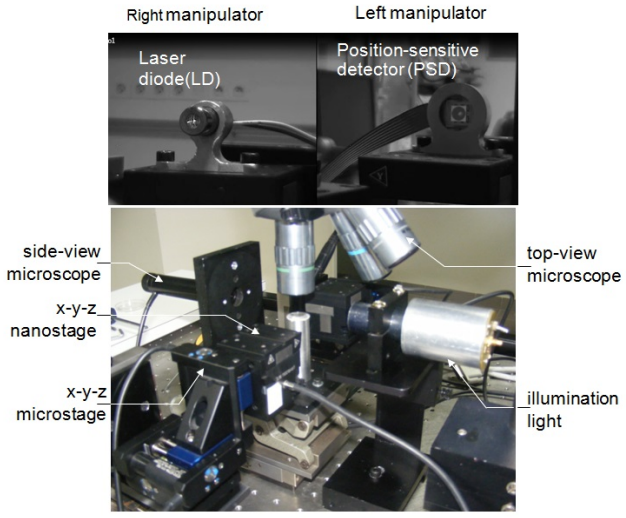

Fig. 2. Experimental setup.

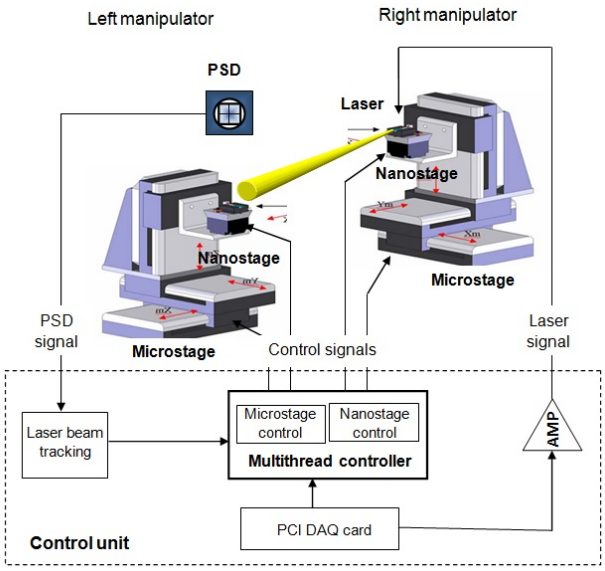

Fig. 3. Schematic diagram of the architecture of the laser beam tracking control system.

II. Experimental Setup

The experimental setup of the beam pointing and tracking system is depicted in Fig. 2. Two controllable micro/nano manipulators facing each other, composed of 3 degree of freedom (dof) high-precision dual-stages, i.e., magnetic x-y-z closed-loop microstage (MCL Nano-Bio2M on the x-y-z axes) and piezoelectric x-y-z closed-loop nanostage (P-611.3S NanoCube from Physics Instruments), respectively. The coarse motion of the microstage is about few centimeters and the fine motion of the nanostage is about $100 \times 100 \times 100 \mu$m positioning and scanning range comes in an extremely compact package. The laser source is mounted on top of the nanostage (right manipulator) producing the laser beam. The main components of the beam steering experiment are a 635 nm laser. A four-quadrant position sensing device (PSD) mounted on top of the nanostage (left manipulator) that measures the position of the image that the laser beam forms on a fixed plane. On the side view, a white light illuminates the workspace for top-view (optical microscope – Mituyo $\times 50$) and side-view (digital microscope – TIMM $\times 150$) imaging. The sample platform is at rest during manipulation that is fixed on the system base.

Fig. 9 shows the overall control scheme for power, laser beam tracking and micro/nano manipulator control. The laser beam motion control (brownian or stochastic trajectory) and measurement sequences are processed in real-time using MATLAB™xPC software with a stand alone target machine operating at a sample-and hold rate of 2kHz. A data acquisition (DAQ) (NI 6289) card is used for highspeed capturing of photodiode voltage output from a lock-in to detect laser beam intensity maximum and beam tracking. A multi-thread planning and control system is developed to independently manage the coordination during parallel laser beam motion and tracking, respectively.

III. Dynamics Modeling

This section reviews the different model dynamics of the different system components.

A. Dynamics of Piezoelectric and Magnetic Actuators

The first step for controller synthesis is to set up dynamic modeling. Because we have no parametric information on drivers of the dual micro/nano stages composed by piezoelectric 3-dof nanostage and the magnetic 3-dof microstage (that are deemed as three-input and two-output system), the modeling approach is based on system identification using Pseudo Random Binary Sequence input signal. The dynamic models of the micro and nano-stages are formulated respectively by the following estimated discrete transfer functions:

$$\begin{aligned} G_{m(x,y,z)}(z) &= \frac{b_0 + b_1 z^{-1} + b_2 z^{-2} + b_3 z^{-3}}{1 + a_1 z^{-1} + a_2 z^{-2} + a_3 z^{-3}} \\ G_{n(x,y,z)}(z) &= \frac{b_1 z^{-1} + b_2 z^{-2} + b_3 z^{-3}}{1 + a_1 z^{-1} + a_2 z^{-2} + a_3 z^{-3}} \end{aligned} \quad (1)$$

These models are constructed to match the dynamic response of the system with a reduced order and obtain a third-order approximation. Furthermore, to ensure high precision tracking process of the laser beam motion, a cooperation between the micro/nano-stages is mandatory. Hence, the tracking output signal generated by the dual micro/nano stages is considered as the sum of their respective position outputs following the master/slave strategy with a decoupled structure proposed in Section 4.

B. Dynamics of Four Quadrant Photo Sensitive Detector

A four quadrant photo sensitive detector (PSD) has four photosensing parts arranged in four quadrants, respectively.

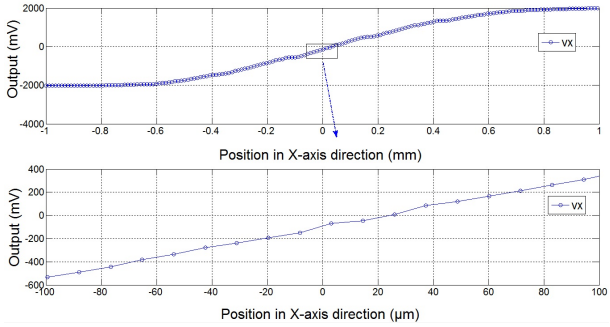

Fig. 4. Output voltage curve V_x with a zoom in the block area near zero on an four-quadrant PSD.

When the elements are lighted by a beam of laser, they will generate currents according to the light intensity and then amplified into voltage signals.The combinations of voltages V_1 to V_4 can be used to indicate the offsets of the spot in relation to the center of the PSD as follows:

$$\begin{aligned} V_x &= (V_1 + V_4) - (V_2 + V_3) \\ V_y &= (V_1 + V_2) - (V_3 + V_4) \\ V_s &= V_1 + V_2 + V_3 + V_4. \end{aligned} \tag{2}$$

The V_x and V_y channel outputs are directly related to the energy of the laser beam that falls in each quadrant while V_s is the sum voltage. It is assumed that the light intensity on the laser's beam cross section obeys Gaussian distribution. The current generated by each sensing element can be described as given in:

$$I = k_1 \iint \frac{2E_l}{\pi^2 r} e^{\frac{2(x_1^2+y_1^2)}{r^2}} dx_1 dy_1 \tag{3}$$

where I is the current, r the radius of the laser light spot, E_l is the energy of the laser beam, (x_1,y_1) is the coordinate of a point on the light spot in a coordinates system located at the center of the light spot, and k_1 is a coefficient. As shown in Fig.4, in the operation region (small neighborhood of the aligned location), the photodiode voltage output V_x is approximately linearly related to light intensity units, with a negative slope. As the curve V_y is similar to that, it is omitted here. Obviously, when the spot is located in the sensing surface $V_x \neq 0$, $V_y \neq 0$ while if the spot is located in the center $V_x = 0$, $V_y = 0$.

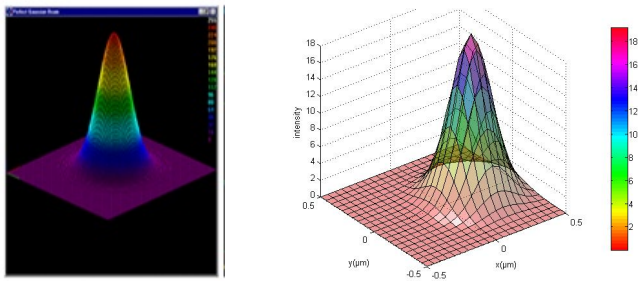

(a) (b)

Fig. 5. Light intensity on the laser's beam cross section: (a) theoretical and (b) experimental intensity obeying to Gaussian distribution.

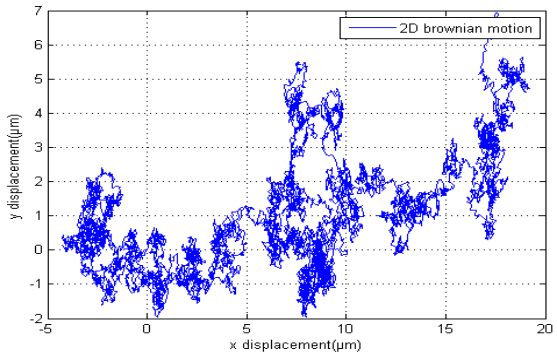

Fig. 6. Particle Brownian motion

As we can see in Fig.5, the experimental intensity sensed by the PSD can be fitted with a Gaussian distribution as calculated by the theoretical Eq. (3).

C. Dynamics of Laser Beam Position

The laser beam motion is assumed similar to the brownian motion (represented in Fig. 6) of a particle subjected to excitation and frictional forces. The brownian motion is given by the generalized differential equation:

$$\frac{d^2x(t)}{dt^2} + \beta_x \frac{dx(t)}{dt} = W_x \tag{4}$$

were β_x coefficient of friction and $W_x \sim N(0, \delta_x^2)$. To estimate with a discrete filter the laser beam positions at each sampling time t_k, a discrete model of the continuous dynamic (4) is necessary. In the x-coordinate the discredited equations of motion using a zero-order hold (zoh) are given by:

$$\dot{x}_k = \frac{x_k - x_{k-1}}{\Delta T} \tag{5}$$

$$\ddot{x}_k = \frac{\dot{x}_k - \dot{x}_{k-1}}{\Delta T} \tag{6}$$

from (4) and (6) we obtain :

$$\dot{x}_k = a_x \dot{x}_{k-1} + b_x W_{x_k} \tag{7}$$

where ΔT is the discretisation time step and the statistic properties of the excitation force W_{x_k} is assumed to be an zero-mean Gaussian random variable with variance δ_x^2 and a_x, b_x are constant parameters identified in the x-axis. The y-axis can be modeled in the same manner as the x-axis, though with different dynamics. For 2D representation, the source state at discrete time k is defined as

$$[x_k \ y_k \ \dot{x}_k \ \dot{y}_k]^T \tag{8}$$

(x_k, y_k) and $(\dot{x}_k, \dot{y}_k)$ are the source position in the plane x-y and velocity respectively. The discrete state space of the brownian laser beam is represented by:

$$X_k = AX_{k-1} + BW_k \tag{9}$$

$$Y_k = CX_{k-1} \tag{10}$$

with

$$A = \begin{bmatrix} 1 & 0 & \Delta T & 0 \\ 0 & 1 & 0 & \Delta T \\ 0 & 0 & a_x & 0 \\ 0 & 0 & 0 & a_y \end{bmatrix}, \; B = \begin{bmatrix} 0 & 0 & b_x & 0 \\ 0 & 0 & 0 & b_y \end{bmatrix}^T$$

$$C = \begin{bmatrix} 1 & 0 & 0 & 0 \\ 0 & 1 & 0 & 0 \end{bmatrix}$$

The state representation matrices$(A,\ B)$ are derived from the particle dynamics defined in (5)-(7), and $W_k \sim N(0, Q)$ is an zero-mean Gaussian random variable with matrix variance Q. It comes from Eq. (9) that:

$$X_k = \sum_{i=1}^{k} A^{k-i} B W_i + A^k X_0 \tag{11}$$

Because successive random variables W_i form *a priori* discrete zero mean white Gaussian process, X_k from Eq. (11) is Gaussian if the knowledge on X_0 is assumed Gaussian or equal to some fixed value. Its *a priori* variance at each step k can be calculated:

$$\sigma^2(X_k) = \sum_{i=1}^{k} A^{k-i} B \sigma^2(W_i) + A^k \sigma^2(X_0) \tag{12}$$

Eq. (12) shows that bigger is the variance of W_k to set and bigger is the *a priori* uncertainty variance on the possible values of the modeled unknown position of the beam laser at t_k. Finally, the measurement Y_k of position takes into account the discrete-time white Gaussian noise V_k and variance R added by the PSD, that is:

$$Y_k = C X_{k-1} + V_k \tag{13}$$

IV. Control Scheme of Beam Pointing and Tracking

The problem considered is that of tracking a laser beam into the x-y plane by robust control issues of the dual micro/nano manipulators motions, and the localization of the current laser beam position [8]. It implies to integrate a prediction-estimation model that anticipates the *a priori* laser beam motion, taking into account both dynamics of the beam laser and manipulators models.

A. Decoupled Control Structure

One of the main characteristics of the dual-stage controller resides on the two control outputs, namely from the micro and the nano controller outputs. However, the main constraint considered here is the different system dynamics of each considered stage. Indeed, the microstage has a large motion range with a low bandwidth, while the second nanostage has a high bandwidth with small motion range. Secondly, the destructive effect, in which these two actuators fight each other by moving in opposite direction, must be avoided. Thus, the control strategy must coordinate the micro/nano-stage to track the laser beam efficiently by using only the position feedback retrieved from the PSD. The master-slave control design allows to transform the dual-stage control design problem into a decoupled or a sequential multiple independent controller designed separately. Fig. 7 illustrates the block diagram of the dual-stage controller using the decoupled control structure. The position error tracking will be compensated by the high bandwidth fine actuator for high precision. The coarse actuator will follow the fine actuator to prevent its saturation.

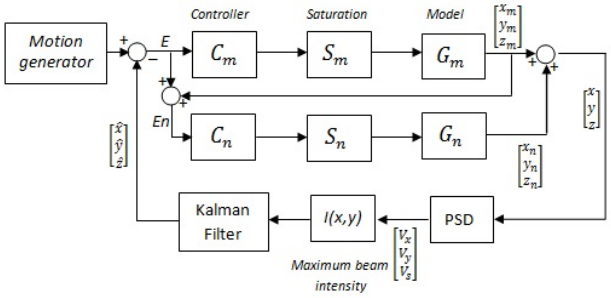

Fig. 7. Master-slave controller with decoupling structure for maximum light tracking.

From the the block diagram depicted on Fig. 7 the total dual-stage open loop transfer function is:

$$G_T = C_n G_n + C_m G_m + C_n G_n C_m G_m \tag{14}$$

and the total closed loop sensitivity function equals the product of the micro/nano-stage loop sensitivities, S_M, S_N respectively, that is:

$$S_T = \frac{1}{1 + G_T} = S_n S_m \tag{15}$$

where

$$S_n = \frac{1}{1 + C_n G_n}, \text{ and } S_m = \frac{1}{1 + C_m G_m}. \tag{16}$$

This demonstrates the possibility to design the performances of each stage (defined by their sensitivity functions) for the overall control synthesis.

B. Kalman Filter Estimator

In robotics, the Kalman filter (KF) is most suited to problems in tracking, localization, and navigation, and less so to problems in mapping. This is because the algorithm works best with well-defined state descriptions (positions, velocities, for example), and for states where observation and time-propagation models are also well understood. The prediction-estimation stages of the KF are derived from Eq. (9) and (13):

a) Prediction: A prediction $\widehat{X}_{k|k-1}$ of the state at time k and its covariance $P_{k|k-1}$ is computed according to:

$$\widehat{X}_{k|k-1} = A\widehat{X}_{k-1|k-1} + BU_k \tag{17}$$

$$P_{k|k-1} = AP_{k-1|k-1}A^T + Q_k \tag{18}$$

b) Update: At time k, an observation Y_k is made and the updated estimate $\widehat{X}_{k|k}$ of the state X_k, together with the updated estimate covariance $P_{k|k}$, is computed from the state prediction and observation according to:

$$\widehat{X}_{k|k} = \widehat{X}_{k|k-1} + K_k(Y_k - C_k\widehat{X}_{k|k-1}) \quad (19)$$

$$P_{k|k} = P_{k|k-1} - K_k S_k K_k^T \quad (20)$$

where the gain matrix K_k is given by:

$$K_k = P_{k|k-1}C_k S_k^{-1} \quad (21)$$

where

$$S_k = C_k P_{k|k-1} C_k + R_k \quad (22)$$

is the innovation covariance. The difference between the observation Y_k and the prediction observation $C_k\widehat{X}_{k|k-1}$ is termed the innovation or residual $r(k)$. Thus the input of the KF is the noisy measurement of the laser beam displacement in the x-y direction delivered by the PSD, and $\widehat{X}_k$ is the output of the filter representing the estimation of the displacement at time k.

V. Experiments

A. Laser beam position estimation

First, a parametrization step, based on the experimental results, is performed to get the model parameters of the laser beam motion, and parameters of the Kalman filter (KF) that is used to estimate the position of the laser beam. In this step, the PSD is fixed, and the laser beam is automatically moved until it was detected by the PSD (see Fig. 9). After positioning the laser beam in the PSD center, a synthetic trajectory generated randomly (defined to not exceed the workspace of the PSD) is given to the laser beam for local maximum search. The maximum intensity provided by the PSD is then computed from Eq. (3). The parameters a_x and b_x are identified by using the Eq. (7) describing the brownian motion. The experimental results of the intensity variation of the laser beam sensed by the PSD is presented in Fig.5(b).

The KF parameters, i.e the measurement noise matrix R and process noise matrix Q where chosen as:

$$R = 10^{-4} I_{2\times 2}$$

$$Q = 10^{-2} I_{4\times 4} + \begin{bmatrix} 0 & 2b_x^2 & b_x & b_x \\ 2b_x^2 & 0 & b_x^2 & b_x^2 \\ b_x & b_x & 0 & 2b^3 \\ b_x & b_x^2 & 2b_x^3 & 0 \end{bmatrix}$$

The noise matrices where chosen empirically to achieve the best performance of the filter. Especially, they were defined symmetric, and determined according to the coefficient friction b_x identified previously. The results of laser beam motion prediction using KF are presented in Fig. 8. At first glance, the filter succeed to follow the true trajectories very closely. As illustrated the performances of the KF in terms of precision the filter converge to the real position of the laser beam with a minimal error.

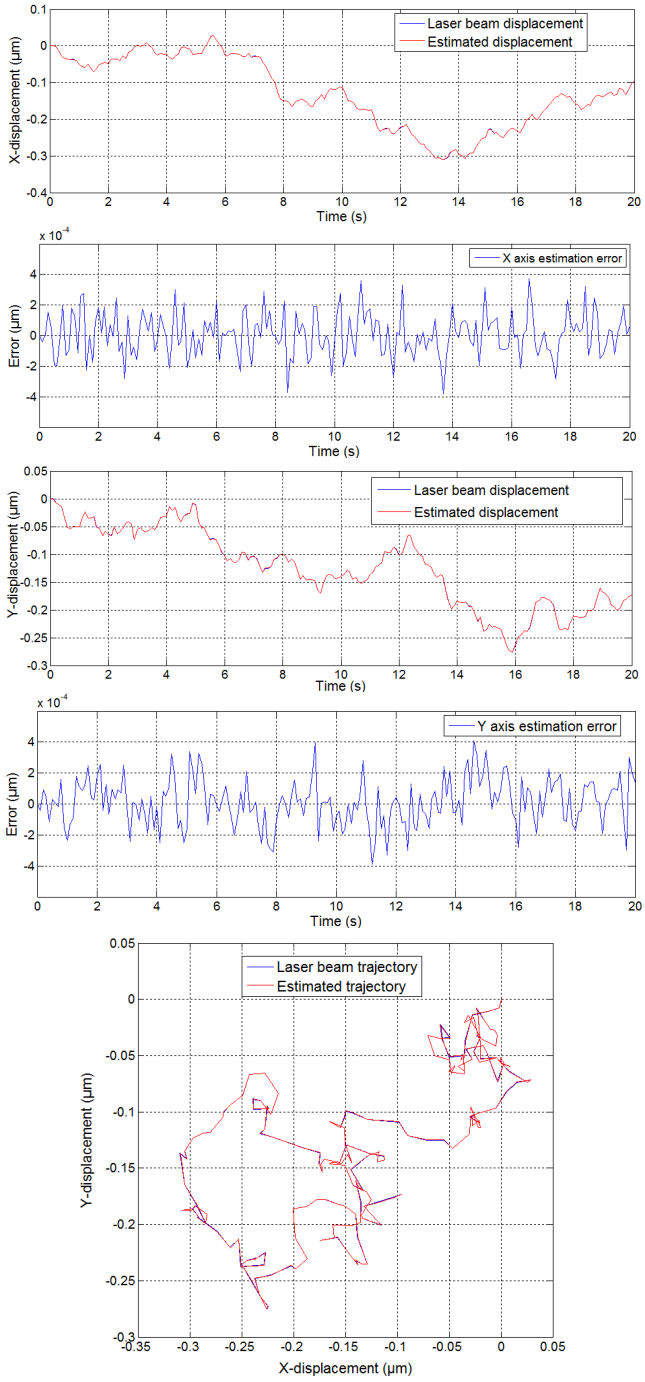

Fig. 8. Laser beam position estimation experiments along x-y axes.

B. Laser beam tracking guided by PSD

In a second step, the efficiency of the KF used for laser beam position estimation, and the control strategy designed to track the laser beam using the PSD are evaluated. To this aim, the laser beam mounted on the right manipulator is moved by a composite signal (constant displacement added by a brownian motion). The results of a typical tracking run is shown in Fig.10 for a fast composite signal sensed by the PSD mounted on the left manipulator. The resulting motion of the PSD is represented in red color while the composite

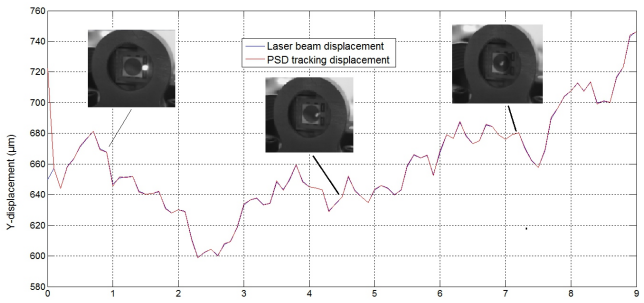

Fig. 9. Laser beam detection of maximum intensity.

reference sent to the right manipulator is represented in blue color. The results demonstrate the robust estimation of the laser beam position in a real time way against brownian perturbations. As expected, the filtered estimate exhibited a smaller variation while the tracking error is lowered (less than few nanometers) leading to very high precision laser beam tracking control. These characteristics are compatible with the laser beam perturbations produced by platform vibrations, piezoelectric actuator thermal drifts, photodetector noises, brownian motion of laser beam and atmospheric turbulence encountered in typical nanomanipulation tasks.

VI. Conclusion

This paper has presented a study of the control problem of a laser beam illuminating and focusing a target subjected to dynamic disturbances using light intensity for feedback only. The main idea is to guide and track the beam with a hybrid micro/nanomanipulator which is driven by a control signal generated by processing the beam intensity sensed by a four-quadrant photodiode. The simulations and experiments demonstrated the efficiency of the approach when submitted to external disturbances. The use of the Kalman filter algorithm for estimating the state of the linear system necessary for implementing the proposed track-following control approach as been proven to be efficient at high dynamics. Further works are undergoing on the implementation of nanomanipulation strategies under the field of view of a focus laser beam to demonstrate the effectiveness of the proposed robust laser beam tracking control.

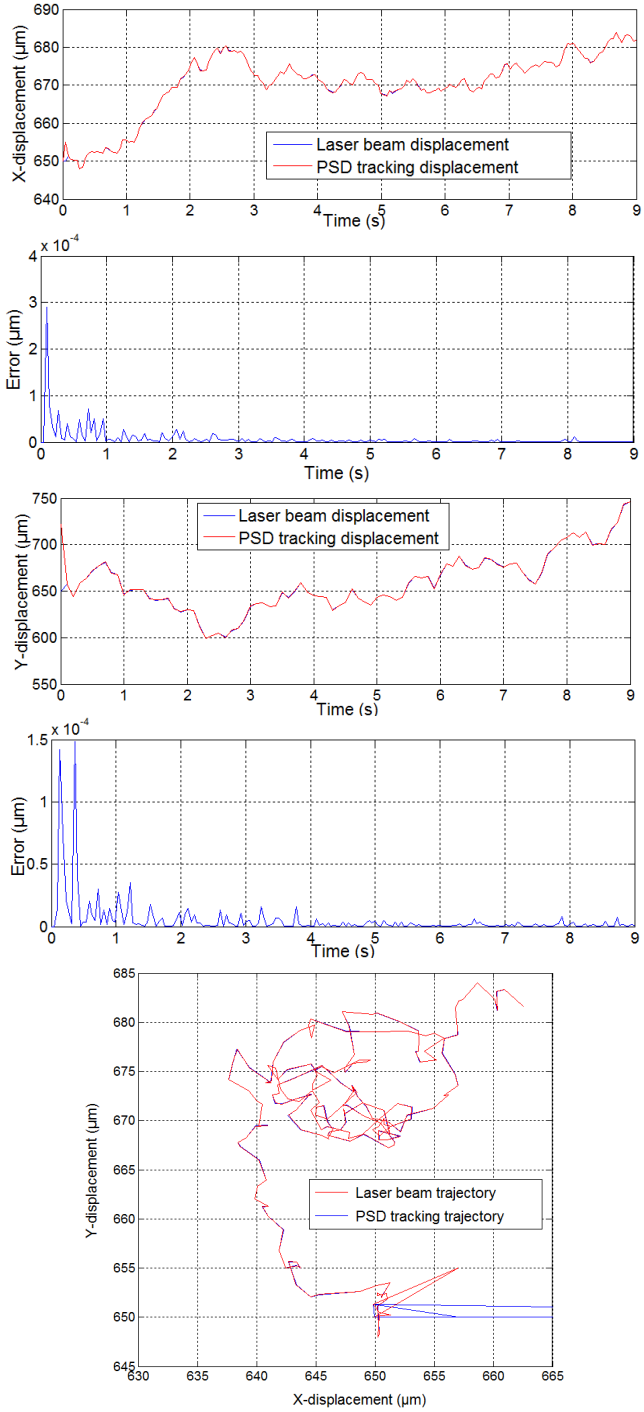

Fig. 10. Laser beam tracking experiments guided by beam intensity of a PSD along x-y axes.

References

[1] A. Ehrlicher, T. Betz, B. Stuhrmann, D. Koch, V. Milner, M. G. Raizen, and J. Ks, Proc. Natl. Acad. Sci. U.S.A. 99, 16024 (2002)

[2] B. Stuhrmann, M. Ggler, T. Betz, A. Ehrlicher, D. Koch, and J. Ks, Automated tracking and laser micromanipulation of motile cells, Rev. Sci. Instrum. 76, 035105 (2005)

[3] H. Xie , S. Rgnier, High-Efficiency Automated Nanomanipulation with Parallel Imaging/Manipulation Force Microscopy, IEEE Transactions on Nanotechnology, Vol.11, Iss.1, pp:21-33, 2012.

[4] Pawel K. Orzechowski, James S. Gibson, Tsu-Chin Tsao, Optimal Disturbance Rejection by LTI Feedback Control in a Laser Beam Steering System, 43rd IEEE Conference on Decision and Control, December 14-17, 2004, Atlantis, Paradise Island, Bahamas, pp. 2143-2148.

[5] C.C. Lee, J. Park, Temperature Measurement of Visible Light-Emitting Diodes Using Nematic Liquid Crystal Thermography With Laser Illumination, IEEE Photonics Technology Letters, Vol. 16, NO. 7, July 2004.

[6] R. B. Evans, J.S. Griesbach, W.C. Messner, Piezoelectric microactuator for dual-stage control, IEEE Transactions on Magnetics, Vol.35, pp.977-981,1999.

[7] Nstor O. Prez-Arancibia, James S. Gibson, and Tsu-Chin Tsao, Observer-Based Intensity-Feedback Control for Laser Beam Pointing and Tracking, IEEE Transactions on Control Systems Technology, Vol.20, No.1, 2012, pp.31-47.

[8] Tran Trung Nguyen, A. Amthor and C. Ament, High Precision Laser Tracker System for Contactless Position Measurement, 2011, in IEEE International Conference on Control System, Computing.